

Photoinduced Electron Transfer in Arylacridinium Conjugates in a Solid Glass Matrix[†]

Guilford Jones, II,^{*,‡} Dingxue Yan,[‡] Jingqiu Hu,[‡] Jiandi Wan,^{‡,§,⊥} Bing Xia,[‡] and Valentine I. Vullev^{*,§}

Photonics Center and Department of Chemistry, Boston University, Boston, Massachusetts 02215, and Department of Bioengineering, University of California, Riverside, California 925521

Received: March 20, 2007; In Final Form: April 16, 2007

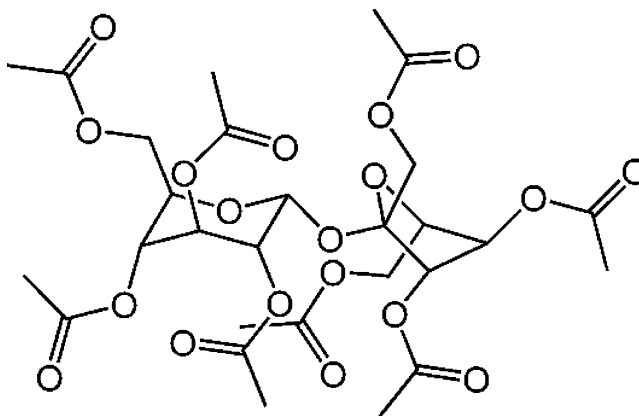
The photophysical properties of a series of 9-arylacridinium conjugates in solid glass matrices composed of sucrose octaacetate have been determined. The fluorescence of the charge-shift states is significantly enhanced because of the retardation of nonradiative pathways for back-electron transfer. Changes of more than 3 orders of magnitude in back-electron-transfer rates (sucrose octaacetate glass vs conventional solvents at room temperature) were observed. Transient spectra displayed long-lived charge-shift species in the microsecond time regime for thianthrene acridinium conjugates. The rate retardation is associated with slow solvation times for surrounding solvent layers in the solid matrix. The red-edge effect (excitation wavelength-dependent fluorescence) for the arylacridinium ions in solid glass confirms the microheterogeneity of the sucrose octaacetate medium.

Introduction

The study of photoinduced reactions in organized media has attracted considerable attention.¹ One purpose of these studies is to mimic processes that occur in biological systems.² Electron-transfer reactions proceed differently in varied environments (e.g., gas, liquid, or solid phase).³ Even in the liquid phase electron-transfer rates are highly dependent upon medium parameters (electronic and nuclear polarizabilities, dipole moments, and relaxation rates). For common solvents, molecules are surrounded by a homogeneous environment in condensed medium, in which maximum solvation can be achieved by the interaction with solvent molecules averaged over many molecular encounters. For a solid solution, the solute and solvent molecules may “freeze” at certain geometries and remain at roughly the same orientation and molecular separation.⁴ Similar behavior could, in principle, be observed for the fluid phase with rapid cooling or with the application of pressure.^{5,6} In addition, medium polarity or effective solvation may change during a cooling process or a phase transition. Since conformational equilibria are severely restricted in the solid phase, unimolecular processes in rigid media tend to be restricted to relatively low-energy conformers,⁷ a situation that is quite different from that present in isotropic liquid phases.

There is growing recognition that electron transfer and other reactions that can be photoinduced for compounds in fluid media can also take place in rigid glasses.^{8,9} Examples that feature intramolecular electron transfer include the investigation of porphyrin-acceptor molecules in glasses of 2-methyltetrahydrofuran at 77 K,¹⁰ ruthenium-ion complexes linked with viologens in alcohol matrices at low temperature and in organic polymers at room temperature,¹¹ and carbazole-acceptor conjugates in thin films composed of a carbohydrate-based polymer, cyanoethy-

SCHEME 1: Structure of Sucrose Octaacetate (SOA)



lated pullulan.¹² Observation of electron transfer or charge migration for reactants dispersed within solid matrices has also been possible for various organic glasses at low temperature under circumstances in which radical anions were produced by pulse radiolysis.^{13,14} A general expectation for systems in glasses is that electron transfer will be retarded in rate because of restrictions placed by the solid medium on the reorganization of solvent dipoles. The limitations on stabilization of developing charge are illustrated in the suppression in the formation of a twisted intramolecular charge transfer (TICT) state for a 4-(*N,N*-dimethylamino)-benzoate moiety and related donor–acceptor chromophores, covalently bound or doped in solid methyl methacrylate copolymers.¹⁵

We have determined that another (nonpolymeric) medium, sucrose octaacetate (SOA), is well suited for formation of room-temperature glasses. Sucrose octaacetate is a readily available derivative of the familiar disaccharide, sucrose (Scheme 1). Its structure, which is composed of two relatively rigid sugar residues adorned with relatively mobile short side chains, has been studied, both for the solid state and for solutions, using NMR or crystallographic techniques.¹⁶ This sucrose derivative has found only limited use in photophysical studies.

[†] Part of the special issue “Norman Sutin Festschrift”.

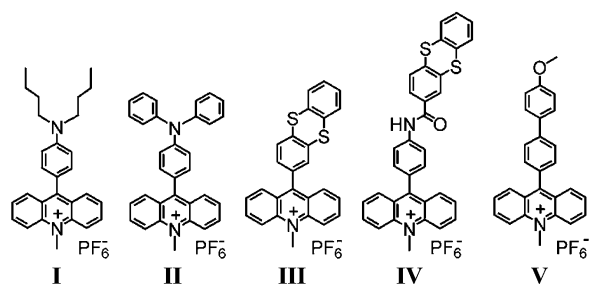
^{*} To whom correspondence should be addressed. E-mail: vullev@ucr.edu.

[‡] Boston University.

[§] University of California.

[⊥] Present address: Division of Engineering and Applied Sciences, Harvard University, 29 Oxford St., Cambridge, MA 02138.

SCHEME 2: Structures of the Acridinium Dyads



Sucrose octaacetate is a white crystalline material that melts at about 83 °C. For the undoped glass, there is no absorption or emission at the wavelengths of interest in photophysical studies (300–800 nm). On rapid cooling from 100 °C, a liquid SOA solution forms a colorless homogeneous glass, which is convenient to handle at room temperature. The relatively high phase-transition temperature of SOA allows us to study systems at room temperature or close-to-room temperatures; that is an advantage over common solvents with phase transition temperatures that can be as low as 100 K.

We have reported the intramolecular electron-transfer properties of conjugates composed of electron donors and 9-acridinium ions.^{17–20} The absorption spectra of these conjugates show (1) a sharp absorption band located at about 360 nm corresponding to the transition between the ground and the locally excited state of the acridinium moiety and (2) a broad band in the visible region that manifests dependence on the solvent polarity and the substituents linked to the acridinium ion. The latter includes transitions from the ground to the charge-shift (CSH) states of the conjugates (i.e., state in which an electron is transferred from the donor to the acridinium moieties). Many of the acridinium-donor conjugates manifest fluorescence from their CSH states. Lappe et al. theoretically investigated the intramolecular charge transfer in some of the 9-aryl-10-methylacridinium conjugates.²¹

Fast photogeneration of long-lived charge-transfer states is essential for the development of artificial light-harvesting systems and optoelectronic materials.²² For two-component donor–acceptor systems, achieving such long-lived states requires suppression of the back-electron transfer or other processes that lead to the decay of the charge-transfer state. Recently long-lived transients were reported for 9-mesityl-10-methylacridinium in liquid media at room temperature.^{23,24} The low reorganization energy of the system placed the back-electron-transfer kinetics in the inverted Marcus region.²³ Photoexcitation of a noncovalent complex containing protonated acridinium ions manifested electron-transfer states that lived for microseconds when in liquid solution at room temperature.²⁵ The electron-transfer state of the same noncovalent complex did not manifest detectable decay when in a solid media at 77 K.²⁵

Here we report a spectroscopic investigation of five 10-methylacridinium conjugates (Scheme 2) in sucrose octaacetate glass. Use of the solid medium resulted in a significant enhancement of the emission of the selected conjugates (~30

to 200-fold increase in the fluorescence quantum yields). When in liquid organic solvents at room temperature, the acridinium donor–acceptor conjugates produced transients with lifetimes in the picosecond time domain; for the solid SOA glass, we observed the formation of charge-shift states that lived for tens and hundreds of microseconds. The rate constants associated with decay to the ground state for photoexcited conjugates doped in solid media manifested non-Arrhenius behavior in the temperature range between 10 and 90 °C, which includes the solid–liquid transition of the SOA matrix. For room-temperature SOA samples, we observed multiexponential emission decays and a “red-edge effect” (dependence of emission on excitation wavelength), revealing inhomogeneity in the conformational distribution of solute molecules “locked” in the solid media.

Results and Discussion

We studied the intramolecular charge-transfer properties of five 9-aryl-10-methylacridinium conjugates (Scheme 2) in solid sucrose octaacetate (SOA) glassy media (Scheme 1). The selected electron donor components were aniline derivatives for I and II, thianthrene moieties for III and IV, and an arylmethoxy derivative for V (Scheme 2).

Absorption Properties of Arylacridinium Conjugates in Solid SOA Glass. As previously reported for liquid media,^{17–19} the absorption spectra of each of the conjugates showed a sharp band at about 360 nm, corresponding to the transition to the local-excited (LE) state of the acridinium moiety, and a broad featureless band in the visible region that includes transitions to the charge-shift (CSH) states of the conjugates (Table 1).

On spectroscopic comparison of conjugates in a liquid ester solvent, ethyl acetate, we observed a noticeable red-shift of 10–20 nm in the CSH absorption maxima for I and II in solid SOA media (Table 1). These trends reflect a higher relative stabilization of the CSH species in the glassy medium owing to, for example, a higher level of solvent destabilization of a more charge-localized ground state. Absorption shifts correspond to changes in energy levels for ground and Franck–Condon (vertical, unrelaxed) excited states.

Alternatively, the negligible media effect on the absorption maxima of III and IV (Figure 1) indicates a lack of stabilization or destabilization effect from the solid matrix on the CSH and ground states of these two conjugates.

Furthermore, we observed negligible differences between the absorption spectra of 9-arylacridinium ions recorded at room temperature (for solid SOA glass) and at temperature that is above the melting point of SOA (for liquid SOA media). The CSH absorption band for 9-arylacridinium conjugates have been shown to be moderately solvatochromic¹⁹ because the energy differences between the ground and CSH excited states depend on solute–solvent interactions. With the assumed moderate polarity for SOA, which is anticipated (a dielectric constant has not been reported for the melt), these changes are expected to

TABLE 1: Absorption and Emission Properties of the 9-Acridinium Conjugates

conjugate	sucrose octaacetate (solid)				ethyl acetate (liquid)				emission enhancement
	$\lambda_a^{(\max)}$ nm	$\lambda_f^{(\max)}$ nm	Φ_f $\times 10^3$	ΔG_f eV	$\lambda_a^{(\max)}$ nm	$\lambda_f^{(\max)}$ nm	Φ_f $\times 10^3$	ΔG_f eV	
I	584	680	38	– 1.8	569	500	0.20	– 2.5	190
II	547	660	64	– 1.9	535	500	0.40	– 2.5	160
III	427	500	22	– 2.5	426	488	0.43	– 2.5	51
IV	434	525	260	– 2.4	433	521	2.0	– 2.4	130
V	436	555	100	– 2.2	430	490	3.4	– 2.5	29

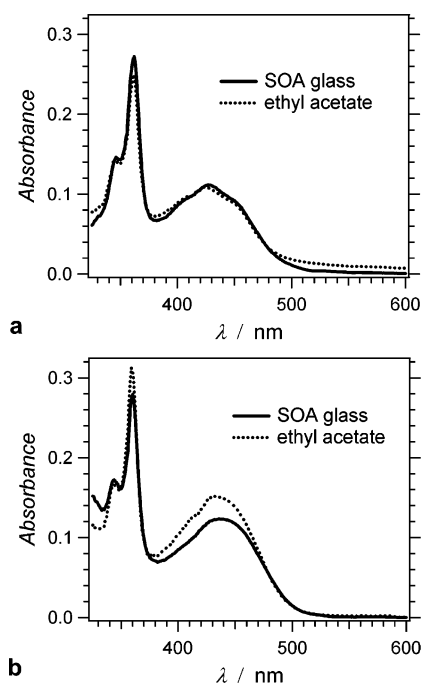


Figure 1. Absorption spectra of (a) III ($20 \mu\text{M}$) and (b) IV ($20 \mu\text{M}$) in a solid matrix (SOA glass) and a liquid solution (ethyl acetate) at room temperature.

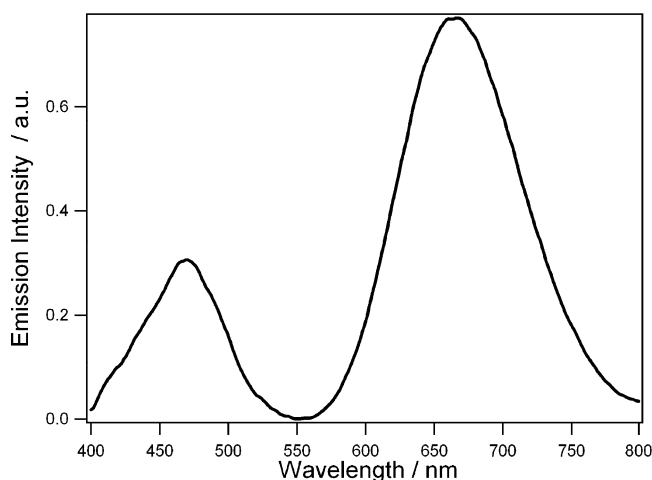


Figure 2. Fluorescence spectrum for II ($20 \mu\text{M}$) in SOA recorded at room temperature, $\lambda_{\text{ex}} = 355 \text{ nm}$. The spectrum shows the emission bands from the locally excited-state of the acridinium moiety ($\lambda_{\text{f}}^{(\text{max})} = 460 \text{ nm}$) and from charge-shift state of the dyad ($\lambda_{\text{f}}^{(\text{max})} = 660 \text{ nm}$).

be slight (e.g., for the melt vs the SOA glass and for SOA vs other moderate polarity solvents). In addition, other differences among media may reflect different degrees of ion-pairing as well as a differential (inhomogeneous) solvation of unassociated cations.

Steady-State Fluorescence Properties of Arylacridinium Conjugates in Solid SOA Glass. We observed a significant fluorescence enhancement for the acridinium conjugates in solid SOA glass in comparison to their emission observed for liquid solutions (Table 1). When excited in the UV region, most arylacridinium conjugates in solid SOA displayed two fluorescence bands (Figure 2): a short-wavelength band associated with the LE state (less than $\sim 490 \text{ nm}$) and a long-wavelength band from the CSH state (in the region from 525 to 700 nm depending on the 9-substituent groups). The intensities of the

CSH fluorescence bands were highly dependent on the medium viscosity (i.e., on the temperature of SOA) and usually dominated the LE bands for solid SOA samples. The intensities of the LE fluorescence bands, in contrast, were relatively insensitive to the medium viscosity (i.e., to the liquid vs the solid state of SOA).

From the fluorescence maxima, we estimated the Franck–Condon energy gap for the radiative transition to the ground state: $\Delta G_{\text{f}} = ch/\lambda_{\text{f}}^{(\text{max})}$ (Table 1). Because for solid SOA media the transition from CSH dominates the radiative decay, ΔG_{f} can be approximated to the driving force for the back-electron transfer, $\Delta G_{\text{bet}}^{(0)}$. The values for $\Delta G_{\text{bet}}^{(0)}$ calculated from electrochemical data for the acridinium conjugates (with the assumption that SOA is a medium-polarity solvent) are in a good agreement with the values for ΔG_{f} .

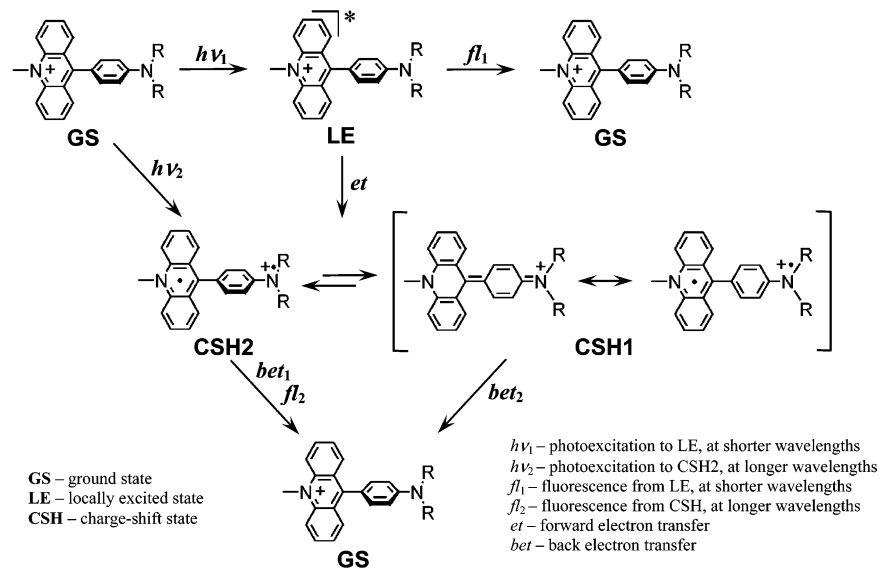
For solid SOA media, the anilinoacridinium ions displayed clearly resolved LE and CSH fluorescence bands (Figure 2). In contrast, for liquid solvents, such as ethylacetate, I and II did not display emission from the CSH state; that is, the fluorescence maxima for these conjugates were at shorter wavelengths than the maxima of their CSH absorption bands (Table 1). Emission from LE states was reduced in intensity as well.

Scheme 3 delineates a proposed mechanism of dual fluorescence encompassing LE state decay to the ground state and forward electron transfer to the CSH state. For a nearly coplanar conformation of CSH1 state, the p orbital of amino nitrogen and the π orbitals of phenyl group are arranged with potential overlap. The nearly coplanar CSH1 may nonradiatively decay rapidly, that is, with strong electronic coupling between donor–acceptor subunits, returning to the ground state via fast back-electron transfer. In contrast, in the twisted conformation for the CSH2 state the p orbital of nitrogen and the π orbitals of phenyl group are arranged nearly orthogonally, and therefore electronic coupling between those orbitals is limited.²⁶ The twisted CSH2 state shows competitive radiative decay to the ground state and displays CSH fluorescence.

On the basis of molecular modeling calculations, the twist angles between the acridinium and the phenyl rings of the most stable conformations are between 60 and 70 degrees for I and II. Presumably, this variety of conformations with different twist angles is similar for the solid phase. Because the rotating motion is restricted in the solid phase, the excited-state conformation for the dye molecule remains similar to that of the ground state. Conformational transitions through a coplanar state, CSH1 (Scheme 3), leading to efficient nonradiative back-electron transfer, will be suppressed in solid media. It can be assumed that those conformations with the pretwist angle near 90° (i.e., greater than $\sim 60^\circ$) might display longer wavelength CSH fluorescence. For a liquid solution, even the conformation with twist angle near 90° , that is, CSH2 states, might undergo rotating motion to deactivate the CSH state, and therefore no CSH fluorescence is observed.

For acridiniums conjugated with thianthrene in nonpolar liquid solvents, we have observed CSH states that are as low as 1.7 eV above the ground state.¹⁸ For solid SOA media, the absorption and fluorescence data did not reveal such low-lying CSH states (Table 1). This finding can be ascribed to (1) the moderately high polarity of SOA, for example, compatible to, or larger than, the polarity of CH_2Cl_2 , resulting in destabilization of the CSH states involving oxidized thianthrene species,¹⁸ and (2) rigidity of the solid media that suppresses the geometrical changes in the thianthrene ring essential for its oxidation, that is, evolution of the nonplanar thianthrene electroneutral group to the planar thianthrene radical cation.^{27,28}

SCHEME 3: Mechanism of Electron Transfer for Aniline Derivatives of Acridinium Conjugates



Time-Resolved Fluorescence Measurements for Arylacridinium Conjugates in Solid SOA. We measured the emission lifetimes of the acridinium conjugates using the phase-modulation technique. The enhancement of fluorescence efficiency for the acridiniums in SOA at room-temperature provided measurable decays. In all cases, however, the phase and modulation data could not be fit to single-exponential functions, the results contrast with the transient absorption and emission decays which were, for the most part, single component lifetimes for acridiniums in liquid solvents.^{18,19}

In order that qualitative trends in lifetimes could be discerned, we assumed that emission lifetime data could be fitted with a small number of exponential functions (physically, an assumption that dozens of conformers “locked” within the glassy matrix could fall into “families” giving rise to similar fluorescence decay behavior). Single-exponential fits, that is, $\alpha \exp(-t/\tau)$, resulted in lifetimes longer than ~ 2 ns, however, with quite low quality of the data fits, for example, $\chi^2 > 10$ (Table 2). Data fits to double and triple-exponential decay functions, that is, $\sum_{i=1}^n \alpha_i \exp(-t/\tau_i)$, $n = 2$ and 3 , however, resulted in values of χ^2 close to 1 (Table 2).

The pattern of the obtained lifetimes is relatively consistent. The acridinium conjugates displayed a primary (larger weighting) long-lived component in the 2–13 ns time domain. Decays for minor components varied somewhat more considerably in the 0.1–1.0 ns range.

Microheterogeneity (the distinction among occupation sites) for glassy media has been previously reported.^{29,30} Our observations confirm that a host of fluorescence species of slightly different environmental constraint is important for the salts in SOA. These heterogeneities could arise from differential solvation (SOA ring and substituent packing and the orientation of glassy solvent dipoles) and steric or spatial demands (and the access to free volume) that affect the geometry of the acridinium ions (or the degree of ion-pairing by PF_6^- counterions).

From the average lifetimes, $\tau_{\text{av}} = (\sum_i \alpha_i \tau_i) / (\sum_i \alpha_i)$ (Table 2), and the fluorescence quantum yields, Φ_f (Table 1), we estimated the radiative, k_f , and nonradiative, k_{nd} , decay rate constants for the five acridinium conjugates (Table 2). With the caveat in mind that rate constants (indeed the quantum yields and lifetimes from which they are calculated) do not represent uniquely correct physical constants but more precisely reflect an “average” over

TABLE 2: Fitting Parameters for the Emission Decays of the Acridinium Dyads in SOA

dyad	τ (ns)	α_i	χ^2	τ_{av} (ns)	$k_f \times 10^{-7}$ (s ⁻¹)	$k_{\text{nd}} \times 10^{-7}$ (s ⁻¹)
I	2.5	1.0	42	2.5	1.5	38
	4.0	0.53	1.7	2.4	1.6	40
	0.6	0.47				
	4.0	0.53	1.4	2.5	1.5	38
	0.6	0.34				
II	0.6	0.09				
	3.9	1.0	29	3.9	1.6	24
	6.1	0.84	1.4	5.2	1.2	18
	0.4	0.16				
	7.4	0.59	1.3	5.2	1.2	18
III	3.2	0.27				
	0.2	0.15				
	7.4	1.0	32	7.4	0.30	13
	14	0.79	1.3	11	0.20	8.9
	1.4	0.21				
IV	15	0.73	1.1	12	0.18	8.2
	2.7	0.20				
	0.6	0.07				
V	6.5	1.0	19	6.4	4.0	11
	7.5	0.97	0.76	7.3	3.6	10
	0.1	0.03				
V	6.3	1.0	18	6.3	1.6	14
	7.6	0.99	1.2	7.5	1.3	12
	0.4	0.01				

an ensemble of ions bound within SOA matrices, a number of fundamental trends in the data can be identified.

Decay times for the “fast” series of aniline-acridinium derivatives are slowed by 3 orders of magnitude for SOA glasses vs solvent media. Picosecond decays ($k_{\text{nd}} \approx 10^{12} \text{ s}^{-1}$) reported for acridinium CSH transients in several solvents^{17,19} are altered for the SOA medium to give rate constants for nonradiative decay (k_{nd}) in the range of 10^8 s^{-1} . The pathway for excited-state deactivation via the CSH intermediate is not in doubt because the fluorescence for I and II in SOA is clearly of the CSH-type. Values of k_{nd} are, therefore, most readily associated with decay of CSH intermediates via back-electron transfer (reverse-charge shift). For the aniline series the retardation in rates cannot be ascribed to an effect associated with a driving force for return electron transfer. The CSH species clearly remain low in energy as indicated by the large red shifts of fluorescence (E_{00} values are in the range of 1.8 eV, not too dissimilar to those found for I and II in acetonitrile and

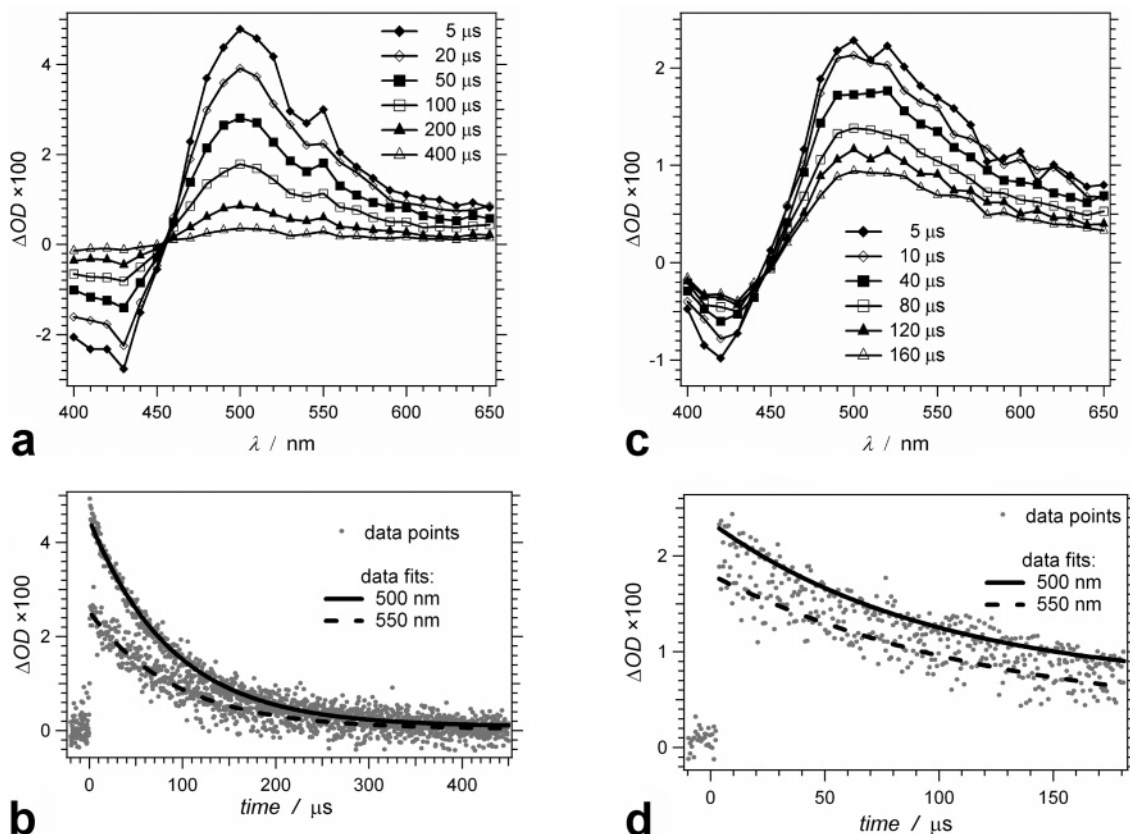


Figure 3. Transient absorption data for III and IV in SOA at room temperature ($\lambda_{\text{ex}} = 355 \text{ nm}$): (a) transient absorption spectra of III ($15 \mu\text{M}$) and (b) the corresponding transient decays for III with monoexponential data fits $\tau_{500 \text{ nm}} = 89 \pm 1 \mu\text{s}$ and $\tau_{550 \text{ nm}} = 93 \pm 3 \mu\text{s}$; (c) transient absorption spectra of IV ($20 \mu\text{M}$) and (d) the corresponding transient decays for IV with monoexponential data fits $\tau_{500 \text{ nm}} = 98 \pm 7 \mu\text{s}$ and $\tau_{550 \text{ nm}} = 124 \pm 22 \mu\text{s}$.

dichloromethane). Since electronic interaction remains strong between acridinium acceptor and donor groups (ϵ_{max} values associated with CSH bands remain strong), prohibition of electron-transfer owing to orbital overlap or related electronic coupling factors is ruled out.

The decay times for the thianthrene series are also considerably extended, approaching 10 ns for III and IV (Table 2). Again, retardation in the nonradiative rate constant, k_{nd} (Table 2), can be evaluated. The conjugates III and IV appear to experience a special “barrier” to electron-transfer that we associate with the thianthrene ring deformation.

Long-Lived CSH Transients. The electron-transfer characteristic for the acridinium derivatives were studied further, using nanosecond laser-flash photolysis methods.³¹ Photoexcitation of III at 355 nm (Figure 3a) yielded transient species at 500 and 550 nm that we ascribed to the reduced acridinium radical and the oxidized thianthrene radical ion, respectively, on the basis of our previous observations at picosecond time domains for liquid solutions.^{18,19,32,33} Flash photolysis of IV resulted in a broader transient at 500–550 nm, indicative of more segregated contributions from the acridine radical and the remotely positioned thianthrene radical ion (Figure 3c). The observed transient absorption from both charge-transfer species in these spectra is consistent with a decoupling of the meso position of the acridine ring, reminiscent of the arrays associated with twisted intramolecular charge-transfer intermediates (TICT) states.^{20,34,35}

Nanosecond laser-flash photolysis measurements did not produce observable transients for the arylacridinium-donor conjugates in liquid media. The decays observed in the microsecond regime for solid SOA media contrast with the picosecond decay

times obtained for transients obtained for organic solvents with different polarities.

Long-lived transients for another acridinium-containing donor–acceptor system, 9-mesityl-10-methylacridinium, have been previously reported.^{23,24} Unlike the compounds investigated in our study, the mesityl-acridinium conjugates do not show charge-shift absorption bands; that is, the absorption and emission spectra of the donor–acceptor conjugate are weighted sums of the spectra of the mesityl and acridinium components.²³ The orthogonal geometry between the two aromatic-ring systems producing this relatively weak donor–acceptor coupling, along with the relatively low reorganization energy, can be the reason for trapping the long-lived mesityl-acridinium CSH states.²³

The rates of decay of the absorption signals from the oxidized donors and reduced acceptors are practically identical for each conjugate and are concurrent with the recovery of the bleaching of the CSH absorption bands at $\sim 420 \text{ nm}$ (Figure 3c,d). Therefore, we assume a mechanism of transient depletion involving simple return of CSH to the ground state via back-electron transfer.

Apparently, the transients living hundreds of microseconds are not representative of the CSH states that undergo emission decay in an average of about 10 nanoseconds. The CSH transients observed with the laser-flash photolysis could be from trapped conformations that require significant solvent reorganization in order to undergo back-electron transfer to the ground state. The very slow rate at which the SOA “solvent” can relax around an altered charge distribution (along a reaction coordinate for the back-electron transfer) will significantly extend the lifetime of these transients. The time scales for solvent relaxation for room-temperature fluid media range widely according to

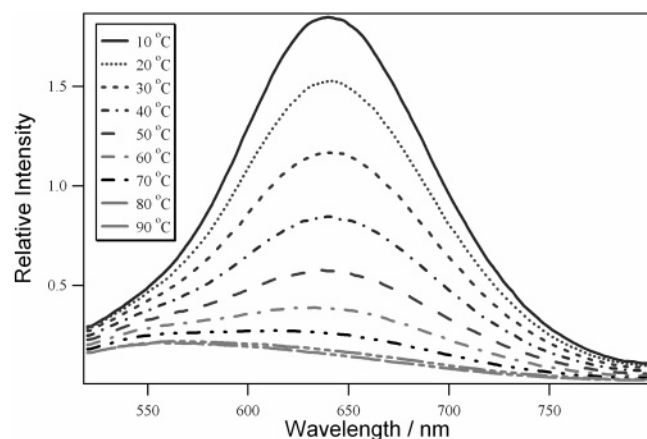


Figure 4. Fluorescence spectra for II (20 μ M) in SOA at different temperatures, $\lambda_{\text{ex}} = 500$ nm.

TABLE 3: Temperature Dependence of the Relative Emission Quantum Yields of the Acridinium Conjugates in SOA

temperature	I	II	III	IV	V
90 °C	0.13	0.16	0.23	0.054	0.070
80 °C	0.16	0.16	0.32	0.054	0.11
70 °C	0.18	0.22	0.45	0.085	0.17
60 °C	0.29	0.31	0.64	0.25	0.28
50 °C	0.45	0.47	0.77	0.47	0.43
40 °C	0.58	0.66	0.91	0.58	0.62
30 °C	0.82	0.91	0.95	0.80	0.83
25 °C	1.0	1.0	1.0	1.0	1.0
20 °C	1.1	1.2	1.0	1.0	1.0
10 °C	1.4	1.4	1.0	1.2	1.2

which kind of physical relaxation is of interest (e.g., fast inertial components < 1 ps, slow “longitudinal” components > 10 ps).³⁶ Solvation dynamics in different confined systems exhibits a dramatically slow component of 100–10000 ps.³⁷ For solids these time scales are extended dramatically since it is the coordinated motion of several solvent layers that is important (not just solvation shells, as with fluids).³⁸

Another possible reason for the long-lived transients could be the formation of a triplet CSH state.²⁰ If the CSH radical states are well segregated, spectrally the triplet and the singlet CSH state will appear similarly. Because of the requirement for intersystem crossing during the intramolecular back-electron transfer, the triplet CSH states, however, will have orders-of-magnitude longer lifetimes than the corresponding singlet CSH states.

Temperature Dependence of the Fluorescence Properties of Arylacridinium Conjugates in Solid SOA. Decrease in the temperature from 90 to 10 °C results in significant enhancement of the fluorescence of the arylacridinium ions in SOA (Figure 4), presumably because of an increase in medium viscosity. Although it melts at 80–85 °C, sucrose octaacetate undergoes its phase transition from liquid to solid glass in the temperature range from 10 to 60 °C. Under practical experimental conditions, sample SOA solution produced a free flowing fluid solution at 90 °C. The profile of cooling was followed by measuring fluorescence quantum yield for the acridiniums as a function of temperature (Table 3). The decays rates manifest a non-Arrhenius behavior that is most profound for III and not as apparent for I and II (Figure 5). For temperatures below ~ 30 °C, the decay rate constant for III in SOA becomes temperature independent. For back-electron transfer such independence of temperature can be due to (1) nearly activationless reaction; that is, $\lambda \approx \Delta G_{\text{et}}^{(0)}$ and $\Delta G^{\ddagger} \ll k_{\text{B}}T$; or (2) the reaction occurs exclusively via nuclear tunneling because $\Delta G^{\ddagger} \gg k_{\text{B}}T$. Assum-

ing that the former as the reason for the observed temperature behavior suggests that the reorganization energy, λ , of III in the solid SOA at room temperature is as high as about 2.5 eV.

The relationships between fluorescence quantum yields for acridinium ions and medium temperature demonstrate the common trend for the arylacridinium ions that the fluorescence efficiencies increase with decreasing medium temperature.³⁹ There has been considerable work done on the effects of the medium viscosity on rate of intermolecular and intramolecular electron-transfer reactions.^{40,41} The common diffusional control intermolecular electron-transfer rate will be limited and determined by medium viscosity, that is, $k_{\text{diffusion}} = 8RT/(3000 \eta)$. The situation is different for intramolecular electron-transfer systems, because the donor and the acceptor are linked in the same molecule (i.e., the donor and acceptor need not undergo diffusional motion). In the present study, the electron-transfer processes could have been influenced by the medium viscosity change (from solution to glass) through two phenomena. The viscosity increase on cooling could have resulted in a decrease in the medium dielectric constant. The trends reported before suggest a slowing of the back-electron-transfer process with reduction in medium polarity. A solvent-polarity effect should have altered the absorption spectra for the highly solvatochromic species, but wavelength shifts were not observed.

Alternatively, the increase in the bulk viscosity with the decrease in the temperature will inhibit the rotating motion of 9-substituents in the acridinium ions. This and other solvent molecular motions are diminished decelerating the nonradiative decay pathways for the acridiniums at lower temperatures.

The “Red-Edge” Effect on Arylacridinium Conjugates in Solid SOA. The fluorescence spectra for arylacridinium ions were not dependent upon the excitation wavelength in fluid medium. In contrast, for SOA glasses the peak wavelengths of fluorescence for the arylacridinium ions were sharply dependent on excitation wavelength (Figure 6). One will observe red-shifts of emission bands if a longer wavelength within the charge shift absorption is utilized for excitation.^{42,43} This phenomenon has been described as the red-edge effect (REE).^{44,45} Observation of REE implies (1) heterogeneity in the microenvironments of the fluorophores and (2) relaxation times of the excited-state that are longer or at least compatible to the emission lifetime. Therefore, REE is readily observed for emission from states with strong charge-transfer character in a highly viscous environment that provides a distribution in the solute–solvent interaction energies.⁴⁵

A potential source for REE is the formation of fluorophore aggregates with various sizes that absorb at different wavelengths; for example, the REE of the solvent fluorescence observed for imidazolium ionic liquids results from such aggregation phenomenon.^{45–48} This is not the case, however, for the REE observed for the CSH fluorescence of the acridinium conjugates. At micromolar concentration range, our observations did not lead us to believe that aggregation was taking place. There was no concentration dependence of the spectral wavelength maxima⁴⁹ or formation of long “tails” at the red edge of the absorption spectra as observed for the ionic liquids.⁴⁵

For a fluid solution, solute molecules are solvated through dipole, H-bond, and other interactions.⁵⁰ If the electronic structure (i.e., dipole moment) of solute is altered upon a transition to another state (e.g., upon photoexcitation from ground to CSH state), a new solvation equilibrium will be reached by reorganization of the surrounding solvent molecules. In a solid matrix, however, not all CSH-excited molecules will experience the

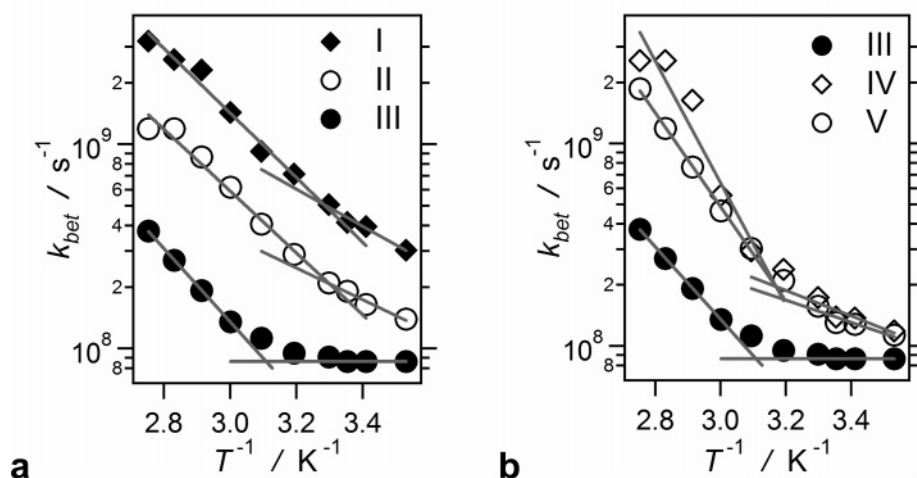


Figure 5. Temperature dependence of the back-electron-transfer rate constant, k_{bet} , for: (a) I, II and III, and (b) III, IV and V in SOA.

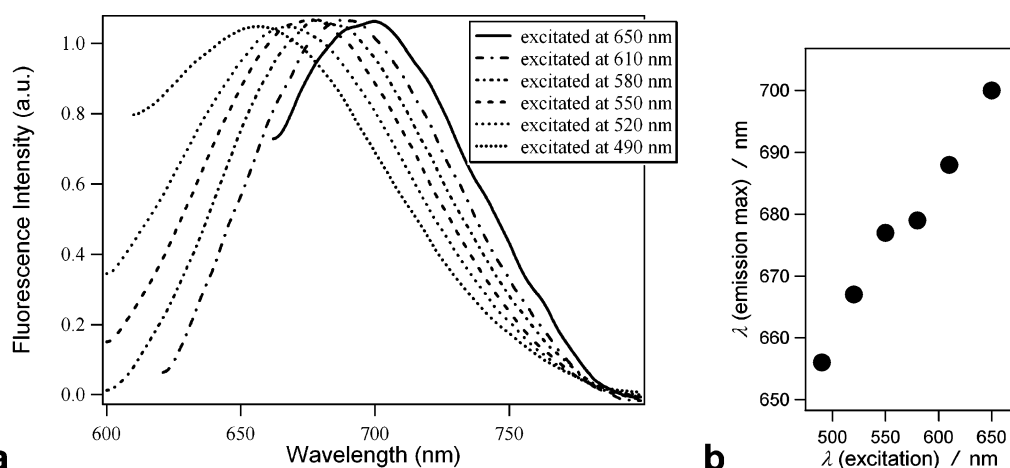


Figure 6. Red-edge-effect for I in SOA glass: (a) normalized fluorescence spectra for I ($10 \mu\text{M}$) in SOA, recorded at room temperature, using various excitation wavelengths; and (b) dependence of the emission maximum on the wavelength of excitation.

completion of such solvent reorganization within the lifetimes of their fluorescent CSH states.

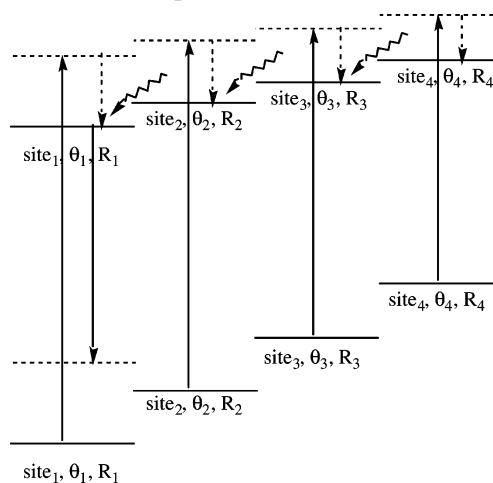
If solutes are “solvated” uniformly following excitation, no REE phenomenon is observed. For the solid state, solute molecules may occupy different microscopic solvation sites in an otherwise macrohomogeneous environment (vide supra). Each site is characterized with a different orientation of the solvent molecules, θ , and intermolecular separations, R , that determine interaction energies. For illustration a variety of hypothetical sites are shown in Scheme 4 representing different interaction energies with particular parameters, θ and R .

Solute molecules at distinct solvation sites give rise to subtly different absorption spectra. In the hypothetical model, the potential energy at different solvation sites increases as the number i increases, shown in Scheme 4. For the acridinium ions excitation results in a decrease of the solute dipole moment giving rise to a strained Franck–Condon state which relaxes along space orientation θ and the transitional coordinator R to the excited-state equilibrium conformation. The emission, however, may occur before these relaxation transitions are completed resulting in different emission wavelengths from the photoexcitation of different θ_i , R_i states.

Conclusions

The fluorescence efficiencies for arylacridinium ions, derivatized with electron donors, are significantly enhanced on

SCHEME 4: Potential Energy Levels for Various Solvation Sites n , ($n = 1, 2, 3, 4$) with Different Orientation θ_i and Separation R_i



dispersion in an SOA glass. For the solid state, the medium viscosity reaches an extreme and restricts conformational freedom and solvent stabilization of charge displacement. The result is an extension of the lifetime of the singlet excited-state for arylacridinium ions to the nanosecond regime. The viscosity of sucrose octaacetate changes dramatically in the experimental

temperature range owing to a liquid-phase \rightarrow solid-phase transition.

The absorption spectra for arylacridinium ions does not change during the SOA phase transition, which illustrates that the ground state of acridinium ion is not influenced by glass formation and that energy gaps among LE, CSH, and ground-state species have not been significantly altered. The intensities for LE emission are less affected by medium temperature (i.e., viscosity) than the CSH intensities; for the latter nonradiative decay processes were dramatically slowed down.

The retardation in rates of back-electron transfer was most noticeable for acridinium ions having aniline substituent groups for which CSH excited states are very low lying (energy gaps for return to ground state are small). For these systems changes of more than 3 orders of magnitude in electron-transfer rate (SOA glass vs conventional solvents at room temperature) could be observed. The rate retardation is associated with slow response times for surrounding solvent layers in the SOA matrix. The dramatic extension of lifetime for high-energy electron transfer intermediates is important to the consideration of utilizing the thermodynamic driving force associated with photoexcitation events for the purpose of multistep charge separation or charge transport in large molecular arrays.

The red-edge effect (excitation wavelength-dependent fluorescence) for the arylacridinium ions in SOA glass confirms the microheterogeneity of the SOA medium. The observation of REE demonstrates that the nuclear motions of acridinium ions and the surrounding matrix are sufficiently restricted in the solid glass that a common equilibrium geometry cannot be reached for a large ensemble of dispersed ions.

Experimental

The arylacridinium hexafluorophosphates were prepared using the procedures described elsewhere.^{18,19,51} The acridinium salts were purified chromatographically followed by consequent recrystallization. The purified compounds have crystalline appearance, and their purity was confirmed with NMR and chromatography.⁵¹ As a result, the conjugates did not contain any impurities that might yield misleading long-lived transient results.⁵² The structures of the acridinium conjugates are shown in Scheme 2.

Sucrose octaacetate (SOA) was purchased (Aldrich) and purified by the following procedure. To remove slightly colored polar impurities, a concentrated SOA chloroform solution (typically 100 g/200 mL) was passed through a short silica gel column (6 cm \times 6 cm) and eluted with more chloroform. After removal of solvent by rotary evaporation, the white powder was recrystallized four times from absolute ethanol and dried in a desiccator at reduced pressure overnight. The purified SOA (white crystals), which had a melting point of 83–85 °C, was stored away from moisture. The purification of SOA is essential for assuring that the long-lived CSH transients (Figure 3) are NOT resultant from external electron donors introduced as impurities of the media.⁵² Ethyl acetate and methylene chloride were analytical grade (Baker). Glycogen was purchased (Sigma) and used directly without purification.

The solid glass samples were prepared for spectroscopic measurements by thoroughly mixing 100 μ L of stock solution (1.0 mM dye in methylene chloride) with SOA powder (9.0 g) and heating the mixture to \sim 100 °C in a small beaker, after which the melt was transferred into 1 cm \times 1 cm quartz cells. The sample was then allowed to cool to room temperature with the cell held in a vertical position to avoid excessive surface

shrinkage. The sample cells were sealed (with Parafilm) from air after cooling and were stored in the dark.

UV–vis absorption spectra were recorded using a Beckman model DU-7 spectrophotometer. Emission spectra were recorded using a model 4800 phase-shift fluorometer from SLM instruments. Fluorescence quantum yield is determined by comparing the spectrally corrected emission intensity of the sample to that of a fluorescence standard. The phase-modulation method was employed for fluorescence lifetime determinations using the SLM 4800 fluorometer.^{53,54} The temperature of sample cuvettes was controlled by a Brinkmann temperature controller, (Lauda model RM6). The temperature range that could be practically used was from –15 to 120 °C. Laser flash photolysis measurements were conducted using a nanosecond laser flash photolysis system equipped with second (532 nm) and third harmonic (355 nm), and with OPO using procedures that have been described.³¹

Acknowledgment. Support of this research by the Department of Energy, Office of Basic Energy Science, Division of Chemistry Sciences, is gratefully acknowledged.

References and Notes

- (1) Ramamurthy, V. *Photochemistry in Organized and Constrained Media*; John Wiley & Sons, Inc.: New York, 1991.
- (2) Sporn, M. B.; Roberts, A. B.; Goodman, D. S., Eds. *The Retinoids*; Academic Press: Orlando, FL, 1984; Vol. 1, 2.
- (3) Chen, P.; Danielson, E.; Meyer, T. J. Role of free energy change on medium effects in intramolecular electron transfer. *J. Phys. Chem.* **1988**, *92*, 3708–3711.
- (4) Marcus, R. A. Theory of charge-transfer spectra in frozen media. *J. Phys. Chem.* **1990**, *94*, 4963–4966.
- (5) Vogel, M.; Rettig, W.; Sens, R.; Drexhage, K. H. Structural relaxation of rhodamine dyes with different N-substitution patterns: a study of fluorescence decay times and quantum yields. *Chem. Phys. Lett.* **1988**, *147*, 452–460.
- (6) Lueck, H.; Windsor, M. W.; Rettig, W. Pressure dependence of the kinetics of photoinduced intramolecular charge separation in 9,9'-bianthryl monitored by picosecond transient absorption: comparison with electron transfer in photosynthesis. *J. Phys. Chem.* **1990**, *94*, 4550–4559.
- (7) Dunitz, J. D., Ed. *X-Ray Analysis and The Structure of Organic Molecules*; VCH: New York, 1995.
- (8) Ramamurthy, V.; Venkatesan, K. Photochemical reactions of organic crystals. *Chem. Rev.* **1987**, *87*, 433–481.
- (9) Thomas, J. M.; Morsi, S. E.; Desvergne, J. P. Topochemical phenomena in organic solid-state chemistry. *Adv. Phys. Org. Chem.* **1977**, *15*, 63–151.
- (10) Gaines, G. L., III; O'Neil, M. P.; Svec, W. A.; Niemczyk, M. P.; Wasielewski, M. R. Photoinduced electron transfer in the solid state: rate vs. free energy dependence in fixed-distance porphyrin-acceptor molecules. *J. Am. Chem. Soc.* **1991**, *113*, 719–721.
- (11) Wasielewski, M. R.; Johnson, D. G.; Svec, W. A.; Kersey, K. M.; Minsek, D. W. Achieving high quantum yield charge separation in porphyrin-containing donor-acceptor molecules at 10 K. *J. Am. Chem. Soc.* **1988**, *110*, 7219–7221.
- (12) Bente, H.; Ohkita, H.; Ito, S.; Yamamoto, M.; Tohda, Y.; Tani, K. Photoinduced intramolecular charge separation in a polymer solid below the glass transition temperature. *J. Chem. Phys.* **2005**, *123*, 084901/084901–084901/084909.
- (13) Miller, J. R.; Beitz, J. V. Long-range transfer of positive charge between dopant molecules in a rigid glassy matrix. *J. Chem. Phys.* **1981**, *74*, 6746–6756.
- (14) Closs, G. L.; Calcaterra, L. T.; Green, N. J.; Penfield, K. W.; Miller, J. R. Distance, stereoelectronic effects, and the Marcus inverted region in intramolecular electron transfer in organic radical anions. *J. Phys. Chem.* **1986**, *90*, 3673–3683.
- (15) Ryu, C. K.; Wang, R.; Schmehl, R. H.; Ferrere, S.; Ludwikow, M.; Merkert, J. W.; Headford, C. E. L.; Elliott, C. M. Photoinduced electron transfer in linked ruthenium(II) diimine-diquat complexes: linkage dependence. *J. Am. Chem. Soc.* **1992**, *114*, 430–438.
- (16) Burgdorff, C.; Loehmannsroeben, H. G. Photophysical properties of tetracene derivatives in solution. III. Thermally activated nonradiative processes and triplet state properties. *J. Lumin.* **1994**, *59*, 201–208.
- (17) Jones, G., II; Farahat, M. S.; Greenfield, S. R.; Gosztola, D. J.; Wasielewski, M. R. Ultrafast photoinduced charge-shift reactions in electron donor-acceptor 9-arylacridinium ions. *Chem. Phys. Lett.* **1994**, *229*, 40–46.

- (18) Jones, G., II; Yan, D.-X.; Gosztola, D. J.; Greenfield, S. R.; Wasielewski, M. R. Photoinduced Charge Migration in the Picosecond Regime for Thianthrene-Linked Acridinium Ions. *J. Am. Chem. Soc.* **1999**, *121*, 11016–11017.
- (19) Jones, G., II; Yan, D.-X.; Greenfield, S. R.; Gosztola, D. J.; Wasielewski, M. R. Anilide Linker Group as a Participant in Intramolecular Electron Transfer. *J. Phys. Chem. A* **1997**, *101*, 4939–4942.
- (20) van Willigen, H.; Jones, G., II; Farahat, M. S. Time-Resolved EPR Study of Photoexcited Triplet-State Formation in Electron-Donor-Substituted Acridinium Ions. *J. Phys. Chem.* **1996**, *100*, 3312–3316.
- (21) Lappe, J.; Cave, R. J.; Newton, M. D.; Rostov, I. V. A Theoretical Investigation of Charge Transfer in Several Substituted Acridinium Ions. *J. Phys. Chem. B* **2005**, *109*, 6610–6619.
- (22) Holten, D.; Bocian, D. F.; Lindsey, J. S. Probing Electronic Communication in Covalently Linked Multiporphyrin Arrays. A Guide to the Rational Design of Molecular Photonic Devices. *Acc. Chem. Res.* **2002**, *35*, 57–69.
- (23) Fukuzumi, S.; Kotani, H.; Ohkubo, K.; Ogo, S.; Tkachenko, N. V.; Lemmetyinen, H. Electron-Transfer State of 9-Mesityl-10-methylacridinium Ion with a Much Longer Lifetime and Higher Energy Than That of the Natural Photosynthetic Reaction Center. *J. Am. Chem. Soc.* **2004**, *126*, 1600–1601.
- (24) Benniston, A. C.; Harriman, A.; Li, P.; Rostron, J. P.; Van Ramesdonk, H. J.; Groeneveld, M. M.; Zhang, H.; Verhoeven, J. W. Charge Shift and Triplet State Formation in the 9-Mesityl-10-methylacridinium Cation. *J. Am. Chem. Soc.* **2005**, *127*, 16054–16064.
- (25) Tanaka, M.; Ohkubo, K.; Gros, C. P.; Guillard, R.; Fukuzumi, S. Persistent Electron-Transfer State of a p-Complex of Acridinium Ion Inserted between Porphyrin Rings of Cofacial Bisporphyrins. *J. Am. Chem. Soc.* **2006**, *128*, 14625–14633.
- (26) Cooley, L. F.; Han, H.; Zimmt, M. B. Evaluation of Electronic Coupling in a Donor-Bridge-Acceptor Molecule: A Fluorescence Polarization Anisotropy Investigation. *J. Phys. Chem. A* **2002**, *106*, 884–892.
- (27) Fronza, G.; Ragg, E.; Ronsisvalle, G. Conformation of thianthrene and 2,7-dichlorothianthrene partially oriented in a nematic phase. *J. Chem. Soc., Perkin Trans. 2* **1982**, 1209–1211.
- (28) Distefano, G.; Galasso, V.; Irgolic, K. J.; Pappalardo, G. C. The dipole moment and helium(I) photoelectron spectroscopic study of the conformations of chalcathrenes. *J. Chem. Soc., Perkin Trans. 2* **1983**, 1109–1112.
- (29) Hamity, M.; Senz, A.; Gsponer, H. E. Luminescence quenching of Ru(bpy)₃²⁺ by nitrophenols in silicate thin films. *J. Photochem. Photobiol., A* **2006**, *180*, 9–14.
- (30) Bonzagni, N. J.; Baker, G. A.; Pandey, S.; Niemeyer, E. D.; Bright, F. V. On the origin of the heterogeneous emission from pyrene sequestered within tetramethylorthosilicate-based xerogels: a decay-associated spectra and O₂ quenching study. *J. Sol-Gel Sci. Technol.* **2000**, *17*, 83–90.
- (31) Vullev, V. I.; Jones, G., II. Nanosecond laser flash photolysis: Dealing with dynamic-range and response-time limitations of the detection system. *J. Appl. Sci.* **2005**, *5*, 517–526.
- (32) Jones, G., II; Huang, B.; Griffin, S. F. Electron-transfer, photochemistry of thianthrene. Nucleophile-assisted photooxidation to sulfoxide. *J. Org. Chem.* **1993**, *58*, 2035–2042.
- (33) Jones, G., II; Huang, B. Photoactive peptides: development of a redox catalytic triad for sulfide oxidation based on poly-L-histidine. *J. Phys. Chem.* **1992**, *96*, 9603–9605.
- (34) Jones, G., II; Farahat, M. S. Photoinduced electron transfer in flexible biaryl donor-acceptor molecules. *Adv. Electron Transfer Chem.* **1993**, *3*, 1–32.
- (35) Jones, G.; Jimenez, J. A. C. Azole-linked coumarin dyes as fluorescence probes of domain-forming polymers. *J. Photochem. Photobiol., B* **2001**, *65*, 5–12.
- (36) Barbara, P. F.; Jarzaba, W. Ultrafast photochemical intramolecular charge and excited state solvation. *Adv. Photochem.* **1990**, *15*, 1–68.
- (37) Bhattacharyya, K. Solvation Dynamics and Proton Transfer in Supramolecular Assemblies. *Acc. Chem. Res.* **2003**, *36*, 95–101.
- (38) Suib, S. L. Luminescence as a probe of porous solids. *Photochem. Photophys.* **1991**, *3*, 1–48.
- (39) Ephardt, H.; Fromherz, P. Fluorescence and photoisomerization of an amphiphilic aminostilbazolium dye as controlled by the sensitivity of radiationless deactivation to polarity and viscosity. *J. Phys. Chem.* **1989**, *93*, 7717–7725.
- (40) Osborne, A. D.; Winkworth, A. C. Viscosity-dependent internal conversion in an aryl-substituted rhodamine dye. *Chem. Phys. Lett.* **1982**, *85*, 513–517.
- (41) Khoshtariya, D. E.; Dolidze, T. D.; Neubrand, A.; Van Eldik, R. Ionic and hydrogen bonding dynamics coupled to optical and thermal electron transfer: temperature, pressure and viscosity effects. *J. Mol. Liq.* **2000**, *89*, 127–146.
- (42) Al-Hassan, K. A.; El-Bayoumi, M. A. Edge-excitation red-shift of the fluorescence of flexible solute molecules that may assume different geometries. *Chem. Phys. Lett.* **1986**, *123*, 39–41.
- (43) Al-Hassan, K. A.; Azumi, T. The red edge effect as a tool for investigating the origin of the anomalous fluorescence band of 9,9'-bianthryl in rigid polar polymer matrixes. *Chem. Phys. Lett.* **1988**, *150*, 344–348.
- (44) Demchenko, A. P.; Sytnik, A. I. Solvent reorganizational red-edge effect in intramolecular electron transfer. *Proc. Natl. Acad. Sci. U.S.A.* **1991**, *88*, 9311–9314.
- (45) Samanta, A. Dynamic Stokes Shift and Excitation Wavelength Dependent Fluorescence of Dipolar Molecules in Room Temperature Ionic Liquids. *J. Phys. Chem. B* **2006**, *110*, 13704–13716.
- (46) Mandal, P. K.; Samanta, A. Fluorescence Studies in a Pyrrolidinium Ionic Liquid: Polarity of the Medium and Solvation Dynamics. *J. Phys. Chem. B* **2005**, *109*, 15172–15177.
- (47) Paul, A.; Mandal, P. K.; Samanta, A. On the Optical Properties of the Imidazolium Ionic Liquids. *J. Phys. Chem. B* **2005**, *109*, 9148–9153.
- (48) Paul, A.; Mandal, P. K.; Samanta, A. How transparent are the imidazolium ionic liquids? A case study with 1-methyl-3-butylimidazolium hexafluorophosphate, [bmim][PF₆]. *Chem. Phys. Lett.* **2005**, *402*, 375–379.
- (49) Jones, G., II; Vullev, V. I. Ground- and Excited-State Aggregation Properties of a Pyrene Derivative in Aqueous Media. *J. Phys. Chem. A* **2001**, *105*, 6402–6406.
- (50) Hirschfelder, J. O., Ed. *Intermolecular Forces*; Advances in Chemical Physics, Vol. 12; Interscience: New York, 1967.
- (51) Yan, D. Synthesis and photochemical properties of arylacridinium salts (electron transfer). Ph.D. Dissertation, Boston University, 1997.
- (52) Ohkubo, K.; Kotani, H.; Fukuzumi, S. Misleading effects of impurities derived from the extremely long-lived electron-transfer state of 9-mesityl-10-methylacridinium ion. *Chem. Commun.* **2005**, 4520–4522.
- (53) Jameson, D. M.; Weber, G. Resolution of the pH-dependent heterogeneous fluorescence decay of tryptophan by phase and modulation measurements. *J. Phys. Chem.* **1981**, *85*, 953–958.
- (54) Jameson, D. M.; Gratton, E.; Hall, R. D. The measurement and analysis of heterogeneous emissions by multifrequency phase and modulation fluorometry. *Appl. Spectrosc. Rev.* **1984**, *20*, 55–106.